

Prediction of Compressive and Tensile Strength of Asphalt Concrete

A.A.A. Molenaar¹⁺ and N. Li^{1,2}

Abstract: The failure characteristics of asphalt mixtures should be known in order to be able durable pavements. Tension and compression tests performed at a range of strain rates and temperatures are needed in order to obtain a full picture of these failure characteristics. Tension and compression tests are not simple tests and will most probably not be used for practical situations. Therefore a study was initiated at the Delft University to develop a model which allows the tensile and compressive strength to be estimated from mixture parameters. This paper describes the materials tested, the test equipment as well as the model that was derived.

DOI: 10.6135/ijprt.org.tw/2014.7(5).324

Key words: Compression testing; Strength prediction; Tension testing.

Introduction

Cracking, including thermal and fatigue cracking, as well as permanent deformation are major damage modes in asphalt pavements. In order to be able to build durable and sustainable asphalt pavements, the tensile and compressive strength of asphalt mixtures should be known because this knowledge allows Mohr-Coulomb type failure envelopes to be constructed which can be used to analyze whether the occurring stress conditions will cause damage or not. The principle of how such envelopes can be constructed from tension and compression test results and how they can be used in analyzing the occurring stress conditions is shown in Fig. 1 [1]. The ratio Δ_i/Δ_{tot} is an indicator for the number of load repetitions to failure.

This concept has been used to analyze fatigue testing results obtained by means of the 4 point beam bending test (4PB), the uniaxial tension-compression test (UTC) and the indirect tension test (IT) [1]. Test were done in the load controlled mode at 5°C and a frequency of 10 Hz. Two different specimen sizes were used in the IT fatigue test being 100 mm and 150 mm diameter specimens (size 1 and size 1.5). Some results are shown in Fig. 2. The figure shows that the UTC and IT results indicate the existence of an endurance limit which can be indicated as R_{limit} . Furthermore the figure shows that the UTC and IT tests gave the same results and that the IT results were not affected by the specimen size. Size independency was also observed for UTC test results which were obtained with displacement controlled fatigue tests.

The endurance limit values that were derived from the data shown in Fig. 2 were $R_{limit} = 0.2$ for the UTC and IT tests and 0.16 for the 4PB tests. It should be noted that research [1] showed that the endurance limit R_{limit} is dependent on the mode of loading (constant load or constant displacement and temperature; all tests were done at a frequency of 10 Hz).

All in all the research done in [1] showed the importance of the

¹ Road and Railway Engineering, Faculty of Civil Engineering and Geosciences, Delft University of Technology, Stevinweg 1, 2628 CN Delft, the Netherlands.

² Jiangsu Transportation Institute, PR China.

⁺ Corresponding Author: E-mail a.a.a.molenaar@tudelft.nl

Note: Submitted August 7, 2014; Accepted September 6, 2014.

R_A value (Fig. 1) and the failure envelope that can be established by means of tension and compression tests.

Measuring the tensile and compressive strength of materials however is not as simple as it may seem since high demands should e.g. be made on the accuracy of specimen preparation, friction reduction in case of compression testing, stiffness of the testing frame etc. An excellent description of these demands is given in [2]. Furthermore testing is time consuming and costly and therefore a method which would allow to estimate the tensile strength from mixture composition and bitumen properties data would be highly welcomed by practitioners. Such a method would be a valuable addition to existing methods which allow to estimate mixture stiffness and fatigue characteristics [3].

In this paper such a model for predicting the tensile and compressive strength of asphalt mixtures will be presented. Also a description will be given of the test methods used and the mixtures that were tested.

Materials

Uni-axial compression and tension test results of seven different types of mixtures were available for modelling purposes. A short description of those mixtures is given here-after.

- DAC 0/8: Dense asphalt concrete with a 40/60 pen bitumen. The maximum grain size is between 0 and 8 mm [1].

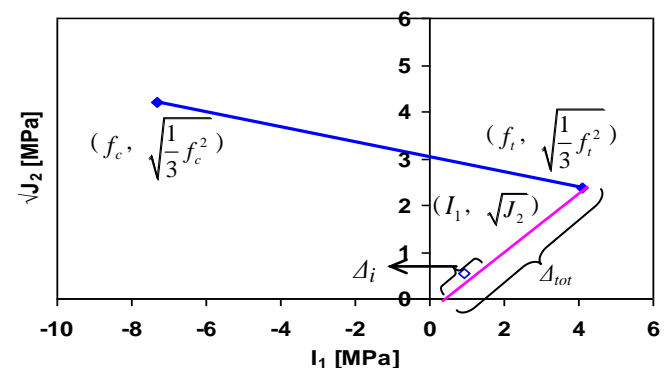


Fig. 1. Yield Surface Determined by Uniaxial Tension and Compression Test Results.

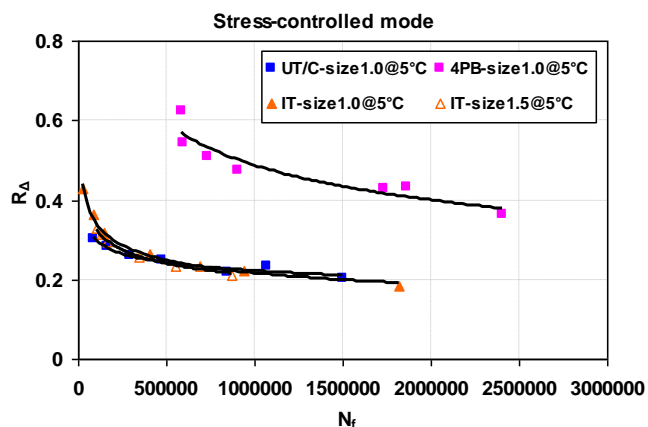


Fig. 2. R_{Δ} vs N_f Relationships for UTC, 4PB and IT Tests Performed in the Load (Stress) Controlled Mode at 5°C and 10 Hz.

- EME 0/14: Enrobé á Modele Elevé, a bituminous base course material with “special” hard binder (10/20 pen). The grain size is between 0 and 14 mm [4].
- PAC 0/16: Porous asphalt concrete with a 70/100 pen bitumen. The grain size is between 0 and 16 mm [5].
- DAC 0/16: Dense asphalt concrete with a 40/60 pen bitumen. The grain size is between 0 and 16 mm [5].
- SMA 0/11: Stone mastic asphalt mixture with a 70/100 pen bitumen. The grain size is between 0 and 16 mm [5].
- ACRé 0/4: A kind of sand mixture with 45/60 pen bitumen. The grain size is between 0 and 4 mm [2].
- GAC 0/32: Gravel asphalt concrete with a 40/70 pen bitumen. The grain size is between 0 and 32 mm [6].

The mixtures were all prepared in the laboratory and virgin materials were used. All specimens except those from the GAC 0/32 and DAC 0/8 mixture were cored from gyrator compacted specimens. The GAC 0/32 and DAC 0/8 specimens were cored from blocks that were compacted using an IPC press box device.

Table 1 is giving some characteristics of the various mixtures. It should be noted that the stiffness modulus reported in Table 1 is determined at a strain rate of 0.1%/s at a temperature of 20°C. Normally mixture stiffness is reported as a function of loading frequency but since it was shown in [7] did show that the stiffness modulus is also dependent on the magnitude of the applied strain it was decided to report the stiffness as a function of strain rate which includes the effects of time of duration of the load (loading frequency) and magnitude of the applied strain. When modulus testing is done at a strain level of $5 \cdot 10^{-4}$, then a strain rate of 0.1% would imply that the modulus is determined at a frequency of 0.5 Hz. Some explanation about this calculation is given hereafter.

All modulus tests were done using a full sine signal with loading time $T = 1/f$ where f is the loading frequency [Hz]. The peak value of the strain is achieved at $t = T/4 = 1/4f$. Although the strain rate is variable when a sinusoidal load is applied the strain rate $d\varepsilon/dt$ is calculated as the ratio of peak strain ε_o divided by $1/4f$ resulting in:

$$d\varepsilon/dt = \varepsilon_o 4f \quad (1)$$

V_a and V_b in Table 1 stand for the volume percentage of aggregates and bitumen respectively. C_c is a parameter

Table 1. Characteristics of the Various Mixtures.

Gradation	E [MPa]	V_a [%]	V_b [%]	C_c
DAC 0/8	5200	3.0	14.9	3.25
EME 0/14	5700	3.4	12.2	0.73
PAC 0/16	2500	20.0	8.2	12.25
DAC 0/16	6900	2.7	12.9	20.48
SMA 0/11	2800	5.2	14.5	0.95
ACRé 0/4	3543	2.6	19.3	0.99
GAC	4700	4.4	8.9	1.60

characterizing the gradation of the mixture. C_c is calculated using Eq. (2).

$$C_c = \frac{D_{30}}{D_{10} \cdot D_{60}} \quad (2)$$

where:

D_{30} : grain diameter at 30 % passing, mm;

D_{10} : grain diameter at 10 % passing, mm;

D_{60} : grain diameter at 60 % passing, mm.

Description of the Test Devices

In this section the compression and tension test set up as used will be described briefly.

Compression Test

When designing and building the uniaxial compression test set-up (see Fig. 3), several influence factors on the state of stress and deformation, such as specimen alignment, frame stability, temperature effect, boundary friction, etc. were considered [2].

The compression test set-up consisted of a 3D-space frame in which an MTS 150 kN hydraulic actuator was mounted. The actuator was rigidly connected to the upper loading plate. The frame itself was placed on an elastically supported concrete block. The load was transmitted from actuator to the specimen through two thin steel plates placed at the top and bottom of the specimen. The bottom and top plate are kept parallel by using three guidance bars (Φ 16 mm) made of Fortal (a strong aluminium alloy), which are connected to the bottom plate and pass through linear bearings in the top plate [2].

Without any precautions at the contact surface between specimen and the loading plates, the radial deformation would be restrained due to the fact that the plates and the specimen have a different ν/E ratio. The resulting friction would act as a confinement for the top and bottom of the specimen, causing the well-known barrel-shape of specimens in compression. To avoid these stress concentration, a friction reduction system was applied to the top and bottom ends of the specimen. The friction reduction system consisted of two thin steel plates and two pieces of rubber, and on both sides of the rubber a thin layer of soft soap was applied. The specimen was placed between two of these metal-soap-rubber-soap sandwiches.

An insulated cabinet with dimensions 0.6×0.5×0.6 m was placed within the frame, which allowed tests to be performed at

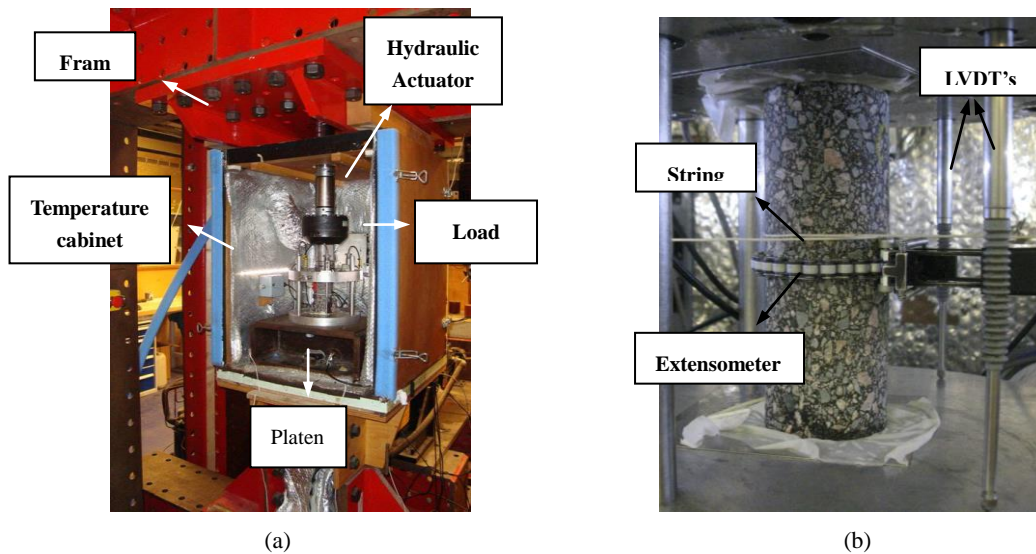


Fig. 3. (a) Compression Test Setup and (b) a Close-up of a Specimen Inside of the Temperature Cabinet.

temperatures ranging between 0 and 45°C with an accuracy of $\pm 0.5^\circ\text{C}$. The cabinet is a sandwich construction of wood and foam. The inside of the cabinet was covered with aluminum/plastic insulation foil. To ensure a uniform temperature distribution throughout specimen, the airflow rate between the upper and lower input channels was adjusted by the two ventilators during the tests, the temperature of the plates and the air were monitored.

The applied force was measured via the MTS load cell, which was positioned between the top plate and the actuator. The axial deformations were recorded by three external displacement transducers (LVDT's) placed vertically to the sides of the specimen. No "on specimen" LVDT's were used because these could be damaged or even destroyed when compression tests were performed at high strain rates and low temperatures. Experience did show that at such conditions sudden, catastrophic, failure was likely to occur causing damage to the LVDT's. The radial deformations at the middle of the specimen were registered by means of two circumferential measurement systems (a string and an extensometer).

The range of the axial LVDT's was ± 20 mm. The string and the extensometer have a range of ± 150 mm and ± 3.75 mm, respectively. The purpose of the extensometer was to enable accurate radial deformation measurements to be made in the initial stages of the test. When the extensometer was out of range, the radial measurements were "taken over" by the string. The measurement systems were connected to a PC-based data acquisition system, which produced a single ASCII output file for each test. The measured data were captured at sampling rates ranging from 1 to 1000 Hz.

Tension Test

The tension test set-up (Fig. 4) consisted of a closed temperature cabinet with a 50 kN hydraulic actuator inside. The actuator was rigidly connected to the bottom of the temperature chamber. In the temperature cabinet the specimen was placed in a rigid framework that could resist the high forces occurring during the tests without

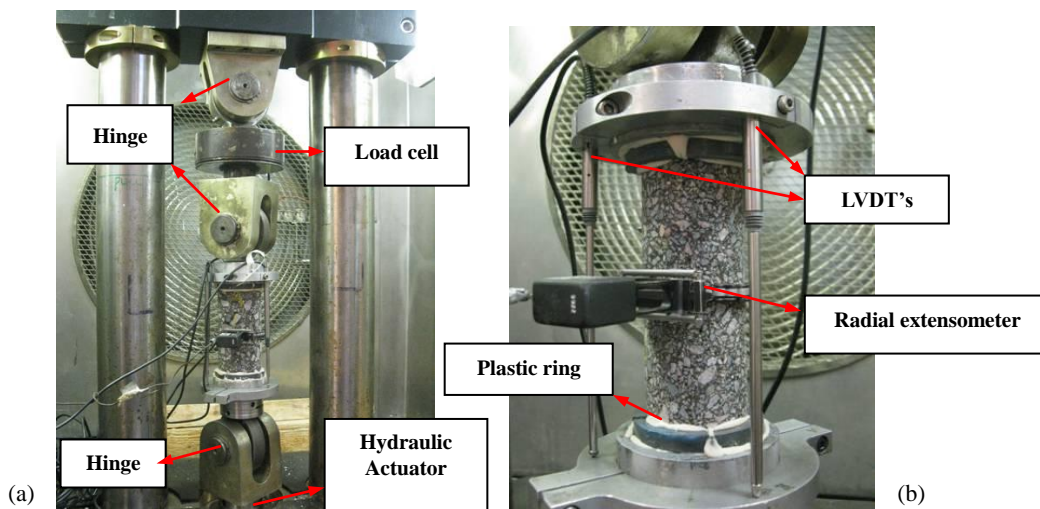


Fig. 4. (a) Tension Set-up and (b) a Close-up of a Specimen Inside of the Temperature Cabinet.

deforming. In the test setup, the specimen was placed between three hinges to ensure that the specimen is subjected to pure uniaxial tension. There were two hinges above and one under the specimen and they avoided bending moments to occur in the specimen. The specimens were glued to the top and bottom end caps using a 2-component fast curing adhesive, X60. This implied that radial deformation at the specimen ends could not occur causing stress concentration near the specimen ends. In order to give a confinement at the ends of the specimen, PVC rings were glued around the specimen ends and the caps to prevent specimens from cracking near the ends.

The force was measured by means of a load cell, which was positioned between the two hinges above the specimen. A 407 MTS controller was used to impose the required controlled deformation rate. The axial deformation was registered by means of three displacement transducers (LVDT's). These LVDT's were fixed in an aluminum ring that was placed around the steel cap at the bottom of the specimen. On top of the specimen, the three LVDT's were positioned such that they touched a second aluminum ring, which was placed around the steel cap on top of the specimen. To obtain an accurate axial displacement curve, LVDT's with a range of ± 1 mm were used for measurements at low temperatures (below 20°C) and high strain rates. LVDT's with a range of ± 5 mm were used at high temperatures (above 20°C) and low strain rates. The measurement systems were connected to a PC-based data acquisition system, which produced a single ASCII output file for each test. Moreover, an oscilloscope was used as a backup for the measurements. A close-up of the tension test set-up with an instrumented specimen is shown in Fig. 4.

Modelling of the Test Results

The unified model, proposed by Medani [7] was used to establish the relationships between material properties and the test conditions; this model is shown in Eq. (3). Based on the Time-Temperature superposition principle, the model allows shifting the data obtained at various temperatures with respect to strain rate at a selected reference temperature. It is believed that when the reduced strain

rate converges to 0 or infinite, the material properties tend to decrease or increase to a limit value [1].

$$P = P_{high} + (P_{low} - P_{high})S \tag{3}$$

where:

$$S = \exp(-[u_r \cdot \beta_T]^\gamma); \quad u_r = \frac{u}{u_0};$$

$$\beta_T = \exp(-T_s [T - T_0])$$

P: a material property e.g. compressive or tensile strength or mixture stiffness [MPa];

P_{low}: value of *P* when *u*→0;

P_{high}: value of *P* when *u*→∞;

u: time derivative variable e.g. strain rate, 1/s;

u₀: reference value of time derivative variable *u*;

β_T: temperature susceptibility function;

T: temperature, K;

T₀: reference temperature, K;

T_s: model parameter, 1/K;

γ: model parameter

The temperature susceptibility factor, *β_T*, of each mixture was determined at a certain reference temperature from the results of mixture stiffness tests.

The theoretical minimum value, *P_{low}*, of the compressive and tensile strength was set to zero since little or no strength and stiffness can be expected at high temperatures and low loading rates without confinement. The other model parameters *P_{high}*, *u₀* and *γ* were obtained by minimizing the differences between the measured and fitted values for all material properties. This procedure was completed by means of the Solver function in Excel. Table 2 summarizes the model parameters that were obtained in this way. Fig. 5 shows how the model was capable of fitting the measured strength values. It was concluded that the model was describing the measured data (very) well.

Table 2. Model Parameters for the Various Mixtures.

	Mixture Type	<i>T₀</i>	<i>T_s</i>	<i>P_l</i>	<i>P_h</i>	<i>u₀</i>	<i>γ</i>	<i>R²</i>
Compressive Strength	DAC 0/8	283.15	0.27	0	48.6	4.37E-02	0.350	0.842
	EME 0/14	283.15	0.27	0	37.1	5.14E-02	0.279	0.840
	PAC 0/16	283.15	0.31	0	18.8	8.61E-02	0.368	0.900
	DAC 0/16	283.15	0.31	0	61.3	9.67E-02	0.315	0.770
	SMA 0/11	283.15	0.33	0	35.1	1.40E-01	0.320	0.919
	ACRe 0/4	283.15	0.30	0	60.6	2.90E-01	0.304	0.937
	GAC 0/32	283.15	0.25	0	50.6	5.40E-02	0.316	0.768
Tensile Strength	DAC 0/8	283.15	0.27	0	6.0	2.25E-04	0.686	0.934
	EME 0/14	283.15	0.27	0	6.0	1.20E-04	0.400	0.852
	PAC 0/16	283.15	0.31	0	2.0	9.83E-04	0.685	0.894
	DAC 0/16	283.15	0.31	0	5.8	2.48E-04	0.569	0.907
	SMA 0/11	283.15	0.33	0	3.9	1.18E-03	0.538	0.943
	ACRe 0/4	283.15	0.30	0	6.1	7.41E-04	0.529	0.957
	GAC 0/32	283.15	0.25	0	4.9	3.07E-04	0.551	0.861

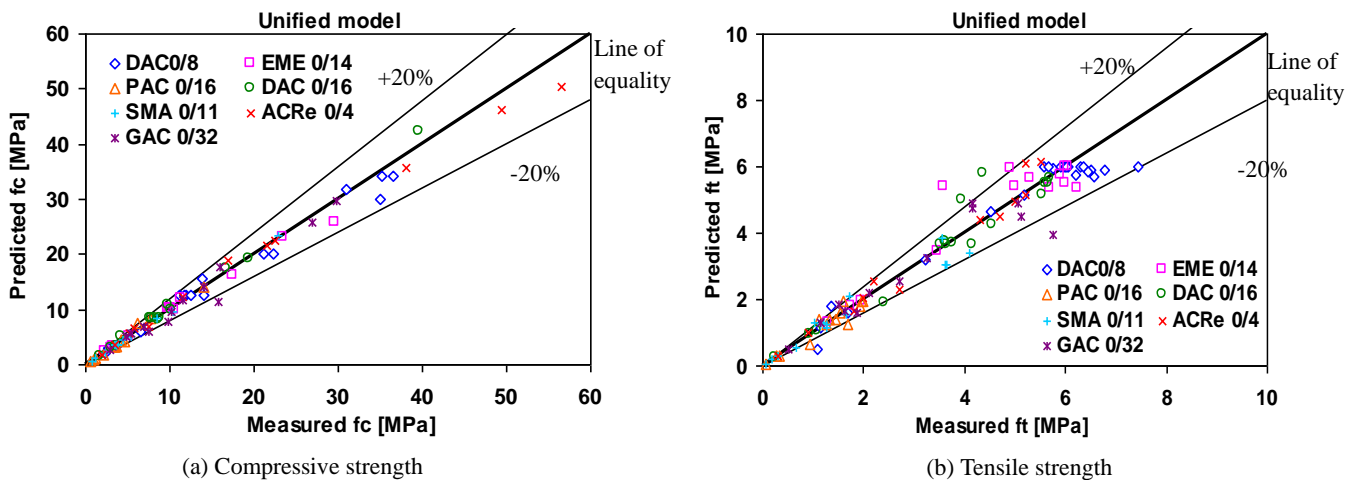


Fig. 5. Measured Strength Values and Those Predicted by the Unified Model.

Model to Predict the Tensile and Compressive Strength of Asphalt Mixtures

The next step in the analysis was the development of a model that was capable of describing the parameters of the unified model using material parameters that are relatively easy to obtain. Heukelom [8] already showed a strong correlation between the stiffness of the bitumen and the strength of the mixture. So it was decided to take the mixture stiffness as an explaining variable. Mixture stiffness however is a factor influenced by the characteristics of the bitumen and the volumetric composition of the mixture. A high stiffness e.g. can be obtained when using a hard bitumen while the void content is still fairly high. Because of this it was decided that the void and bitumen content should be taken as explaining variables as well.

An important parameter in the unified model is P_{high} . Regression analyses were performed to predict the P_{high} of the different mixtures as a function of the mixture stiffness and the volumetric composition. The results of these analyses are given by Eqs. (4), (5) and (6).

$$P_h = a_1 \cdot E^{a_2} \left(\frac{V_b}{V_b + V_a} \right)^{a_3} \tag{4}$$

where:

- P_h : value of P when strain rate $\dot{\epsilon} \rightarrow \infty$;
- E : stiffness at the temperature of 20°C and the strain rate of 0.1 %/s, MPa;
- V_b : volume content of the bitumen, %;
- V_a : volume content of air void, %;
- a_1, a_2 and a_3 : model parameters.

For the compressive strength:

$$P_h = 1.755 \cdot E^{0.402} \left(\frac{V_b}{V_b + V_a} \right)^{0.623} \tag{5}$$

For the tensile strength:

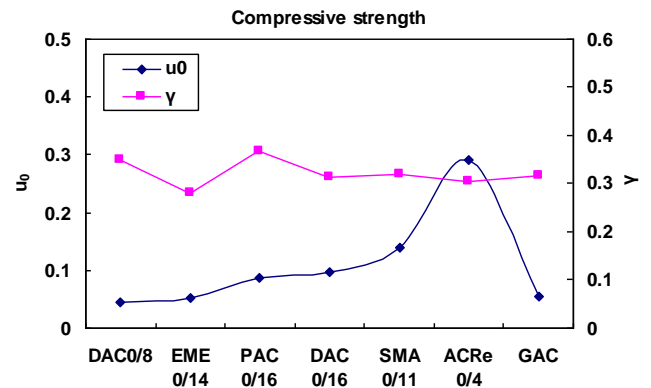


Fig. 6. Parameters u_0 and γ for the Compressive Strength.

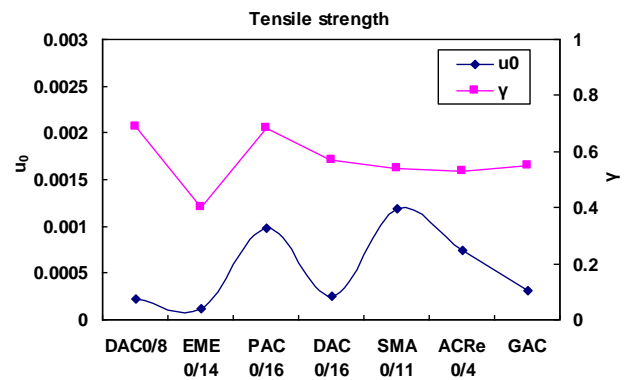


Fig. 7. Parameters u_0 and γ for the Tensile Strength.

$$P_h = 0.505 \cdot E^{0.308} \left(\frac{V_b}{V_b + V_a} \right)^{0.849} \tag{6}$$

Figs. 6 and 7 show that the model parameters u_0 and γ did not vary too much between the different mixtures and therefore it was decided not to develop models to predict u_0 and γ but to use the average value of all the mixtures. This resulted in taking $u_0 = 7.87 \cdot 10^{-2}$ and $\gamma = 0.322$ for predictions of the compressive strength and taking $u_0 = 5.44 \cdot 10^{-4}$ and $\gamma = 0.565$ for the tensile strength predictions.

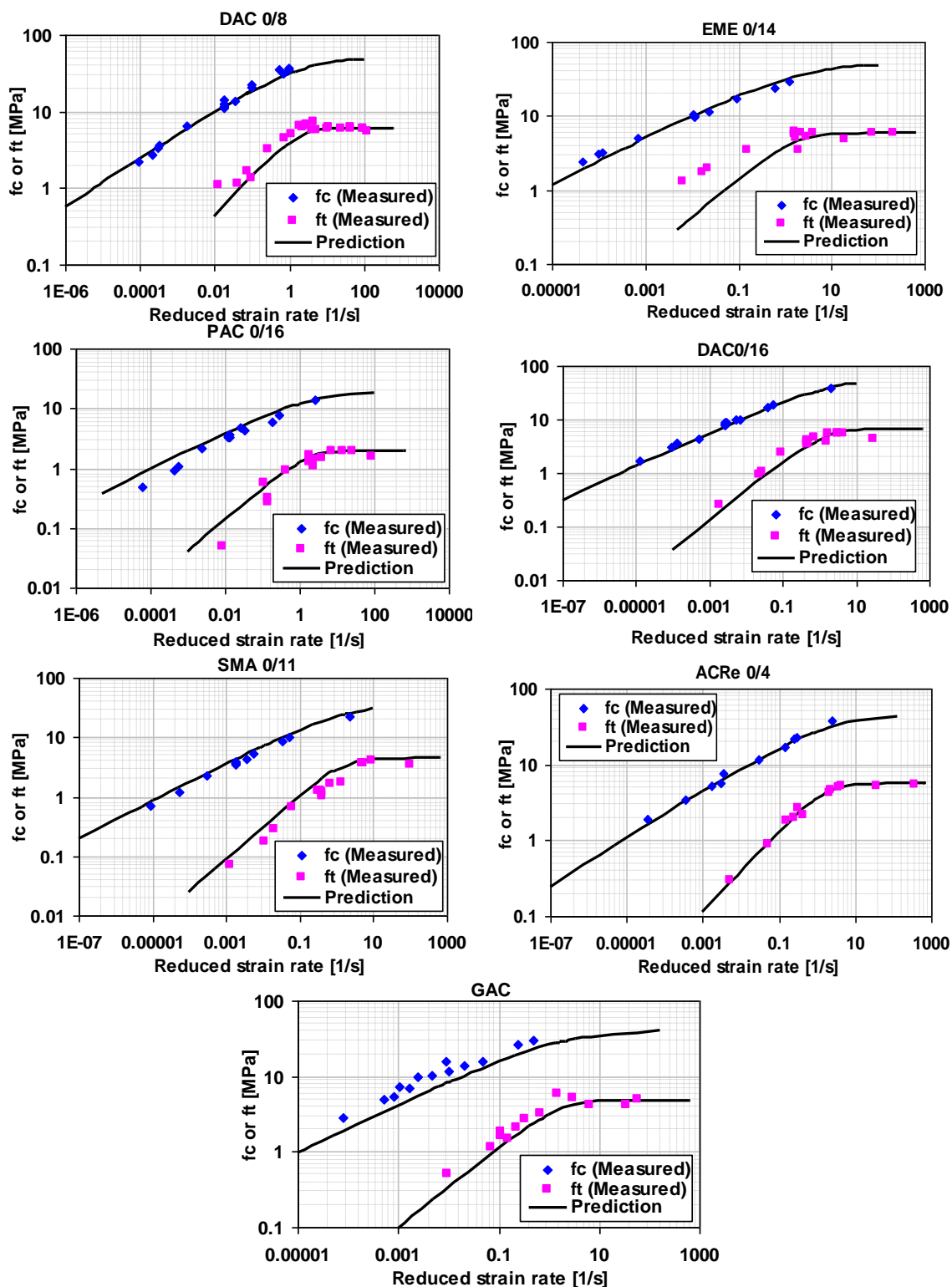


Fig. 8. Prediction of Compressive and Tensile Strength from the Material Properties.

By using Eqs. (5) and (6) as well as the u_o and γ parameter values mentioned above, the tensile and compressive strength of the mixtures was predicted and compared with the measured values. The results are shown in Fig. 8. It can be concluded that the unified model, the parameters of which are estimated in the way described above, predicts the measured values (very) good!

Conclusion

From the results obtained in this study, the following conclusions can be drawn.

- Knowledge about the failure envelop of asphalt mixtures as a function of strain rate and temperature is important for pavement design purposes.

- When the occurring stresses in a pavement are represented by means of the stress invariants I_1 and J_2 then the location of that point in the $I_1 - J_2$ space relative to the failure envelop is a good indicator for, a.o., the fatigue life.
- The failure envelop can be determined by performing tension and compression tests.
- The tension and compression strength can very well be predicted from the model described in this paper which uses mixture stiffness and mixture composition as input.

References

1. Li, N. (2013). Asphalt Mixture Fatigue Testing, Influence of Test Type and Specimen Size, *PhD Thesis*, Delft University of Technology, Delft, the Netherlands.
2. Erkens, S.M.J.G. (2002). Asphalt Concrete Response - Determination, Modeling and Prediction, *PhD Thesis*, Delft University of Technology, Delft, the Netherlands.
3. Shell International Petroleum Company Ltd. (1978). *Shell Pavement Design Manual*, London, UK.
4. Jansen, J.P.M. (2002). Characterising EME Enrobé à Module Elevé, *MSc Thesis*, Delft University of Technology, Delft, the Netherlands.
5. Muraya, P.M. (2007). Permanent Deformation of Asphalt Mixtures, *PhD Thesis*, Delft University of Technology, Delft, the Netherlands.
6. Molenaar, A.A.A., Pramesti, F., and Li, N. (2013). Fatigue Characterisation of Asphalt Mixtures for Designing Long Life Pavements, *Paper presented at the Australian Asphalt Pavement Association Conference*, Brisbane, Australia.
7. Medani, T.O. (2006). Design Principles of Surfacing on Orthotropic Steel Bridge Decks, *PhD Thesis*, Delft University of Technology, Delft, the Netherlands.
8. Heukelom, W. (1966). Observations on the rheology and fracture of bitumens and asphalt mixes, *Journal of the Association of Asphalt Paving Technology*, 35, pp: 358-399.